

PHYSICAL REVIEW LETTERS

VOLUME 68

20 APRIL 1992

NUMBER 16

Scalar Aharonov-Bohm Experiment with Neutrons

B. E. Allman, A. Cimmino, A. G. Klein, and G. I. Opat

School of Physics, University of Melbourne, Parkville, Victoria, 3052, Australia

H. Kaiser and S. A. Werner

Department of Physics and Astronomy, University of Missouri-Columbia, Columbia, Missouri 65211

(Received 3 January 1992)

The scalar version of the Aharonov-Bohm effect predicts a phase shift for de Broglie waves due to the action of a scalar potential in an otherwise field-free (i.e., force-free) region of space. Unlike the more familiar effect due to the magnetic vector potential, the scalar effect has hitherto remained unverified due, presumably, to technical difficulties in electron interferometry. Rather than using electrons acted on by electrostatic potentials, we have performed an analogous interferometry experiment with thermal neutrons subject to pulsed magnetic fields. The expected phase shifts have been observed to a high degree of accuracy.

PACS numbers: 03.65.Bz, 42.50.-p

In classical electrodynamics, potentials are merely a convenient mathematical tool for calculating electromagnetic fields of force. In quantum mechanics, however, potentials have a primary physical significance and are an essential ingredient which cannot be readily eliminated from the Schrödinger equation. In a paper entitled "Significance of Electromagnetic Potentials in Quantum Theory" published in 1959, Aharonov and Bohm [1] proposed two types of actual electron interference experiments aimed at exhibiting these conclusions. The phenomena predicted came to be known as the Aharonov-Bohm (AB) effect, and have given rise to a literature of almost 400 journal articles over the last thirty-odd years.

The essence of the AB experiments [2] is that electrons suffer phase shifts in passing through regions of space of zero fields but nonzero potentials. The effects are of two types, the usual magnetic (or vector) AB effect, and the less often cited electric (or scalar) AB effect which is conceptually quite simple. It concerns the phase shift caused by the scalar potential $V = -eU$ in the Schrödinger equation:

$$(H_0 + V)\psi = i\hbar \partial\psi/\partial t. \quad (1)$$

Figure 1(a) shows a divided electron wave packet traveling down two conducting cylinders which act as Faraday cages, i.e., have a field-free interior irrespective of

their electrostatic potentials U_1 and U_2 . To exhibit the scalar AB effect, the potential of cylinder 2 alone is pulsed during a time when the wave packet is contained inside it. In spite of the absence of a force at all times, a relative phase shift $\Delta\phi$ is expected,

$$\Delta\phi = (1/\hbar) \int eU_2(t) dt. \quad (2)$$

The correctness of this AB prediction is of such importance to the consistency of quantum mechanics [3] that the actual experiment deserves a serious attempt. However, such an experiment has not yet been performed because of technical difficulties with existing types of electron interferometers. The closely related experiment of Mateucci and Pozzi [4] involves forces acting on the electron and is not, therefore, a clear-cut test of the effect. Realizations with protons or ions are hindered by the lack of suitable interferometers for such particles.

In the present experiment with neutrons, the phase shift is due to a scalar potential, $V = -\mu \cdot \mathbf{B}$, which is the analog of $V = -eU$, the scalar potential in the scalar AB effect for electrons. (This parallels a previous situation in which the Aharonov-Casher [5] experiment with neutrons [6] is the analog of the vector AB effect for electrons.)

Consider a split neutron wave packet entering the solenoids in Fig. 1(b). A current pulse $i_2(t)$ is applied

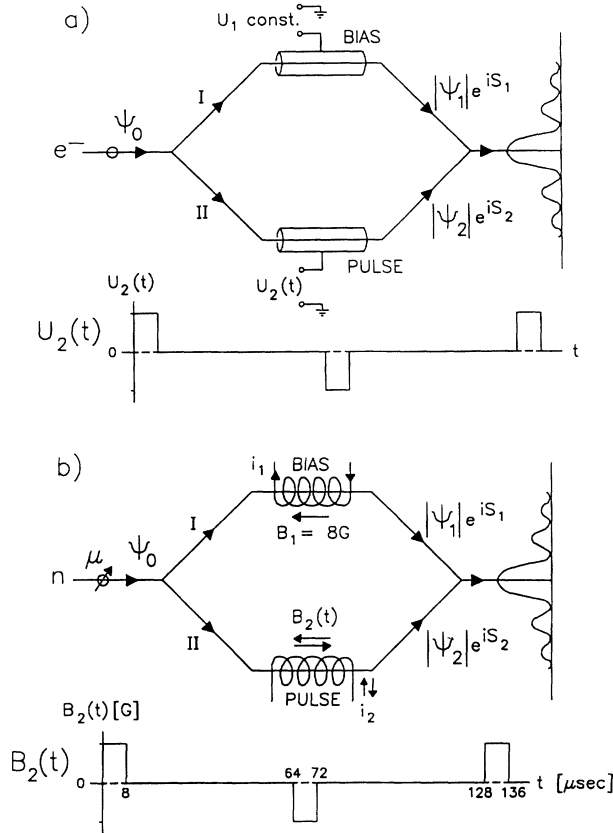


FIG. 1. Schematic diagram of (a) scalar Aharonov-Bohm experiment for electrons and (b) scalar Aharonov-Bohm experiment for neutrons. The wave forms of the applied pulses are also shown.

while the neutron is in the force-free interior of solenoid 2. The resulting magnetic field $B_2(t)$ gives rise to a phase shift,

$$\Delta\phi = (\sigma/\hbar) \int \mu B_2(t) dt, \quad (3)$$

analogously to Eq. (2). In Eq. (3), $\sigma = \pm 1$ depending on whether the neutron is spin up or down relative to the magnetic field, the direction of quantization. In the actual experiment, short duration current pulses, chosen to be $8 \mu\text{s}$ wide, were applied to a suitably designed solenoid placed inside a single-crystal neutron interferometer.

The obvious question that arises is how does one know when to apply the pulses so as to catch the neutrons just as they traverse the center of the solenoid. The equally obvious answer is to apply the pulses cyclically and to gate each detected neutron into a separate scalar according to its arrival time within the cycle. In this way the phase shift of neutrons which traversed the solenoids when the current was zero can be compared with the phase shift of neutrons which traversed the center of the solenoids when the current, and hence the magnetic field, was nonzero.

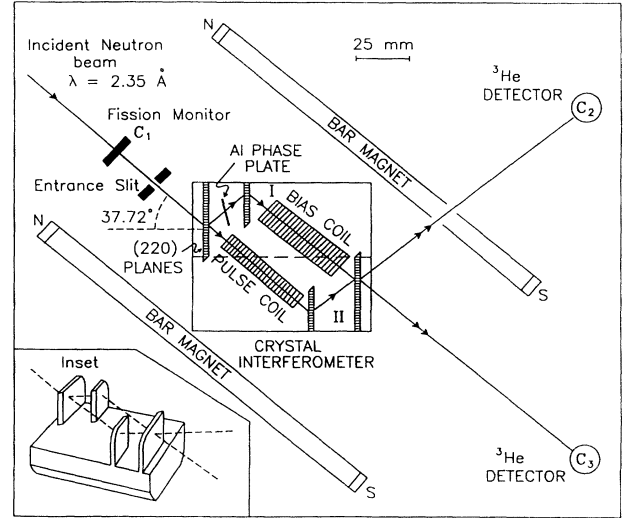


FIG. 2. Layout of AB experiment using a skew-symmetric single-Si-crystal neutron interferometer. Inset: An isometric view of the interferometer crystal.

Another important experimental consideration is the following: Since the phase shift produced by the magnetic fields in the solenoids depends on the relative orientation of the neutron spin, it may appear that the use of polarized neutrons is mandatory. However, by applying a well-defined constant bias field in the second solenoid, one gains separate control over the phase shift for the spin-up and spin-down states thus allowing the AB phase to be measured simultaneously for both, as will be described below.

The experiment, shown schematically in Fig. 2, was carried out at the University of Missouri Research Reactor (MURR), using a collimated, monochromatic neutron beam ($\lambda = 2.35 \text{ \AA}$) incident upon a monolithic, skew-symmetric, perfect-silicon-crystal neutron interferometer [7]. In such a device (see inset in Fig. 2), Bragg diffraction by the (220) planes at the first crystal plate divides the incident de Broglie wave front into two coherent beams. Each of these is deflected by diffraction at the intermediate crystal plates and, after traversing the two solenoids (marked pulse coil and bias coil), the two beams recombine at the last crystal plate. (The whole arrangement is akin to the Mach-Zehnder interferometer of classical optics.)

The quantization direction was aligned with the solenoid axes by means of a rather uniform field, produced by four permanent magnets (each a soft iron bar with neodymium-iron-boron caps) mounted symmetrically around the interferometer.

The counts in the recombined beams, detected by the ^3He counters C_2 and C_3 , are given by

$$N_2 = N_1(a_2 - b_2 \cos \Delta\phi) \quad (4a)$$

and

$$N_3 = N_1(a_3 + b_3 \cos \Delta\phi), \quad (4b)$$

where $\Delta\phi$ is the phase shift of path II relative to path I and N_1 is the count in the monitor counter C_1 . The constants a_2 , a_3 , b_2 , and b_3 characterize the interferometer. (As expected by particle conservation, it is found that $N_2 + N_3$ is independent of $\Delta\phi$, showing that b_2 and b_3 are equal.)

A thin aluminum plate inserted in beam I allowed the phase of the spin-up and spin-down states to be shifted by equal amounts, $\Delta\phi_{AI}$. However, the magnetic field in the bias coil shifts the phase of the spin-up and spin-down states by equal but opposite amounts, $\Delta\phi_m$. Thus, by adjusting both the orientation of the Al plate and the dc current in the bias coil, it is possible to control separately the phase shifts for the spin-up and spin-down states. With these appropriate phases, it is possible to determine the AB phase shift $\Delta\phi_{AB}$ (produced in the pulse coil) with maximum sensitivity even using unpolarized beams.

This may be seen by writing the total phase as

$$\Delta\phi = \Delta\phi_0 - \Delta\phi_{AI} + \sigma(\Delta\phi_{AB} - \Delta\phi_m), \quad (5)$$

where $\Delta\phi_0$ is the offset phase of the interferometer and $\sigma = \pm 1$ for spin up or down. Thus, for an unpolarized incident neutron beam, N_3 is given by

$$\begin{aligned} N_3 = & \frac{1}{2} N_1 \{a_3 + b_3 \cos[\Delta\phi_0 - \Delta\phi_{AI} + (\Delta\phi_{AB} - \Delta\phi_m)]\} \\ & + \frac{1}{2} N_1 \{a_3 + b_3 \cos[\Delta\phi_0 - \Delta\phi_{AI} - (\Delta\phi_{AB} - \Delta\phi_m)]\} \\ = & N_1 \{a_3 + b_3 \cos[\Delta\phi_0 - \Delta\phi_{AI}] \cos[\Delta\phi_{AB} - \Delta\phi_m]\}. \end{aligned} \quad (6a)$$

Similarly,

$$N_2 = N_1 \{a_2 - b_2 \cos[\Delta\phi_0 - \Delta\phi_{AI}] \cos[\Delta\phi_{AB} - \Delta\phi_m]\}. \quad (6b)$$

Rotating the aluminum plate so that $\Delta\phi_0 - \Delta\phi_{AI} = 0(\text{mod } 2\pi)$ and setting the current in the bias coil so that $\Delta\phi_m = \pi/2(\text{mod } \pi)$, we establish a situation such that

$$N_3 = N_1 [a_3 + b_3 \sin\Delta\phi_{AB}] \quad (7a)$$

and

$$N_2 = N_1 [a_2 - b_2 \sin\Delta\phi_{AB}]. \quad (7b)$$

The following experimental procedure was used: (i) With zero bias and pulse fields, $\Delta\phi_{AI}$ was scanned by rotating the aluminum plate. (ii) The bias field was then adjusted until the amplitude of a $\Delta\phi_{AI}$ scan was reduced to zero, thereby setting $\Delta\phi_m = \pi/2(\text{mod } \pi)$. (In fact, the lowest current to achieve this was used, as this minimized the Joule heating which diminishes contrast.) (iii) With the bias field again set to zero, another $\Delta\phi_{AI}$ scan maximized N_3 , so that $\Delta\phi_0 - \Delta\phi_{AI} = 0(\text{mod } 2\pi)$. (iv) The bias field was then returned to the value previously found in (ii). In the actual experiment, the magnetic phase was found to be extremely stable but the spin-independent phase drifted by up to 150 mrad per week and so required reoptimization every few days.

As mentioned earlier, the beam in this experiment was not chopped but the detected neutrons were gated cycli-

cally into a multichannel scaler with 64 channels, each of $2 \mu\text{s}$ width. This was synchronized to the 128- μs period of the current pulses applied to the solenoid. Detectors C_2 and C_3 were accurately positioned to be equidistant from the interferometer exit. Thus, within every cycle, the position of the neutrons at the time of the pulse may be deduced from the known neutron velocity and the time of detection. The finite diameter of the neutron detectors leads to a position uncertainty which corresponds to a time uncertainty of $\approx \pm 1.75 \mu\text{s}$, short compared with the pulse duration and the transit time through the region of uniform field.

The 40-mm-long solenoids wound on hollow formers with two trim coils at each end were computer designed, yielding a field of measured uniformity better than 1% for more than 30 mm on axis, and which decreased rapidly to zero outside. At the de Broglie wavelength of this experiment the neutron speed is 1.68 mm/ μs , yielding more than 17.8 μs of flight time in the uniform region. The 8- μs -wide current pulses (rise time $< 1 \mu\text{s}$) corresponded to 13.5 mm of travel. A field of 21 G [Eq. (3)] yielded a phase shift $\Delta\phi_{AB} = \pi$ rad.

The experimental runs, each lasting about 10 h, consisted of 6×10^8 full cycles of 128 μs . Each cycle contained a positive and a negative 8- μs -wide current pulse, 64 μs apart [Fig. 1(b)]. The results of such a run, in the form of normalized counts in each time delay channel for a typical setting of bias and pulse amplitudes, is shown in Fig. 3. The theoretical curve by which the data are fitted takes into account (i) the actual current pulse shape, (ii) the field distribution inside the coil, (iii) the longitudinal spatial profile of the counter detection efficiency, and (iv) the neutron speed distribution. It is seen to be in excellent agreement with the data.

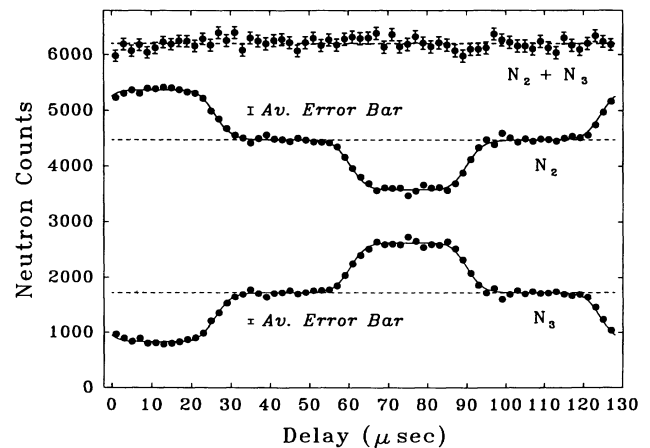


FIG. 3. Scan of counts per channel in the two detectors N_2, N_3 and their sum, plotted against delay time, for the particular case of pulsed field amplitudes of ± 19 G, which corresponds to $\Delta\phi_{AB} = 1.4$ rad. The solid lines are theoretical fits, as described in the text. The total data collection time for this scan was about 10 h.

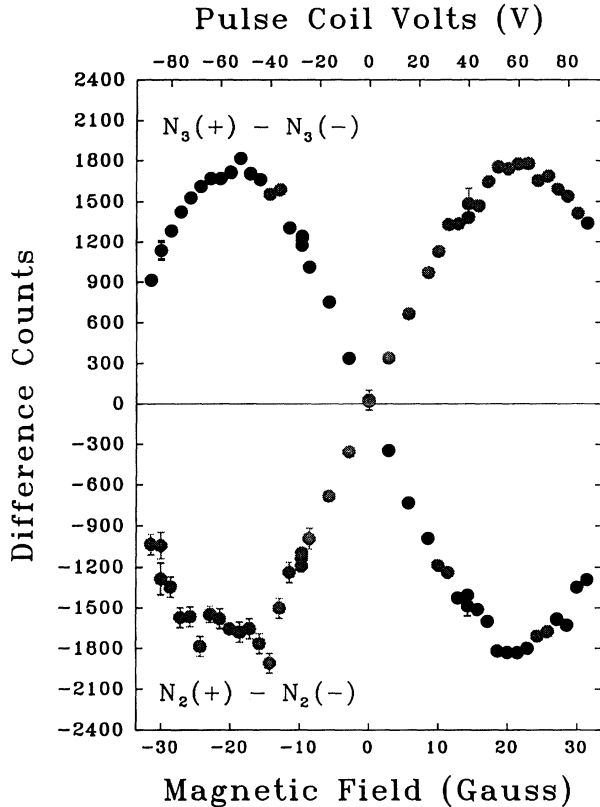


FIG. 4. Interferometer output signals as a function of pulse coil field strengths. This is obtained from the average of the central four points in each plateau region of data sets such as the one shown in Fig. 3. (Certain kinds of systematic error are avoided by taking the difference between the counts for positive and negative pulses.)

A large number of runs were made with increasing values of the current in the pulse coil, corresponding to B fields from 0 to ≈ 30 G ($\Delta\phi_{AB}=0$ to $\approx 3\pi/4$), in the forward as well as the reverse direction. Since all the neutron counts were accumulated cyclically in a multiscalar mode as described earlier, comparison could be made between the neutrons that traversed the solenoid for zero current with those that were within the uniform field of the solenoid for the entire duration of the current pulse (thus experiencing an AB phase shift). The difference in counts between positive and negative polarity pulses,

$$N_3(-) - N_3(+) = 2N_1 b_3 \sin(\Delta\phi_{AB}), \quad (8)$$

displays the expected sinusoidal profile, as shown in Fig. 4, in clear agreement with the AB prediction. The error bars are purely statistical, leaving systematic sources of error for future identification and assessment.

Finally, we wish to refer to earlier experiments in time-dependent interferometry [8] and on Aharonov-Bohm-type experiments with neutrons [9], and to acknowledge valuable discussions with A. Zeilinger, J. Anandan, and J. Spence. This work was supported by the Australian Research Grants Scheme and by the Physics Division, National Science Foundation (Grant No. NSF-PHY-9024608).

- [1] Y. Aharonov and D. Bohm, *Phys. Rev.* **115**, 485 (1959).
- [2] For an exhaustive review, see the monograph by M. Peshkin and A. Tonomura, in *The Aharonov-Bohm Effect*, Lecture Notes in Physics Vol. 340 (Springer-Verlag, Berlin, 1989).
- [3] This was first pointed out in the important paper by W. H. Furry and N. F. Ramsay, *Phys. Rev.* **118**, 623 (1960).
- [4] G. Mateucci and G. Pozzi, *Phys. Rev. Lett.* **54**, 2469 (1985).
- [5] Y. Aharonov and A. Casher, *Phys. Rev. Lett.* **53**, 319 (1984). See also J. Anandan, *Phys. Rev. Lett.* **48**, 1660 (1982); A. G. Klein, *Physica (Amsterdam)* **137B**, 230 (1986).
- [6] A. Cimmino, G. I. Opat, A. G. Klein, H. Kaiser, S. A. Werner, M. Arif, and R. Clothier, *Phys. Rev. Lett.* **63**, 380 (1989). See also H. Kaiser, S. A. Werner, R. Clothier, M. Arif, A. G. Klein, G. I. Opat, and A. Cimmino, *Proceedings of ICAP-12*, AIP Conf. Proc. No. 233, edited by J. C. Zorn and R. R. Lewis (American Institute of Physics, New York, 1991), pp. 247-268; A. S. Goldhaber, *Phys. Rev. Lett.* **62**, 482 (1989).
- [7] For general reviews of neutron interferometry, including references to related experiments, see A. G. Klein and S. A. Werner, *Rep. Prog. Phys.* **46**, 259 (1983), or S. A. Werner and A. G. Klein, in *Methods of Experimental Physics*, edited by K. Skold and D. L. Price (Academic, New York, 1986), Vol. 23, pp. 259-337. See also the conference proceedings, *Matter Wave Interferometry*, edited by G. Badurek, H. Rauch, and A. Zeilinger (North-Holland, Amsterdam, 1988).
- [8] A remotely related experiment on time-dependent interferometry with neutrons is described in G. Badurek, H. Rauch, and D. Tuppinger, *Phys. Rev. A* **34**, 2600 (1986); and with electrons, F. Hasselbach and A. Schäfer, in *Proceedings of the Twelfth International Congress for Electron Microscopy, Seattle, 1990* (San Francisco Press, San Francisco, 1990), Vol. 2, p. 110.
- [9] Other Aharonov-Bohm-type experiments in neutron interferometry are described in D. Greenberger, D. K. Atwood, J. Arthur, C. G. Shull, and M. Schlenker, *Phys. Rev. Lett.* **47**, 751 (1981); A. Zeilinger, M. A. Horne, and C. G. Shull, in *Proceedings of the International Symposium on the Foundations of Quantum Mechanics* (Physical Society of Japan, Tokyo, 1984), p. 289, as well as Ref. [5].

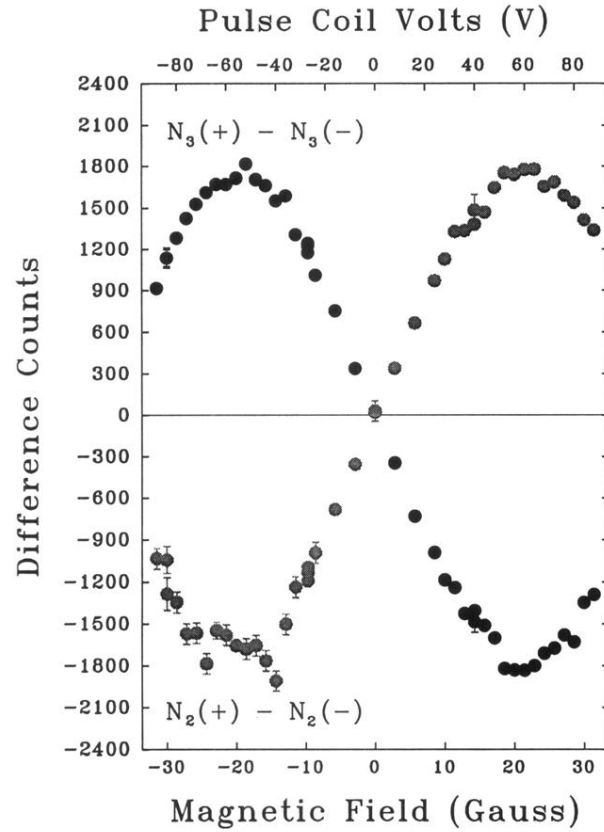


FIG. 4. Interferometer output signals as a function of pulse coil field strengths. This is obtained from the average of the central four points in each plateau region of data sets such as the one shown in Fig. 3. (Certain kinds of systematic error are avoided by taking the difference between the counts for positive and negative pulses.)